

Frequency spectra of absolute optical instruments

Tomáš Tyc^{1,3} and Aaron Danner²

¹ Department of Theoretical Physics and Astrophysics, Masaryk University, Kotlářská 2, 61137 Brno, Czech Republic

² Department of Electrical and Computer Engineering, National University of Singapore, Singapore 117576, Singapore

E-mail: tomtyc@physics.muni.cz

New Journal of Physics **14** (2012) 085023 (16pp)


Received 4 June 2012

Published 29 August 2012

Online at <http://www.njp.org/>

doi:10.1088/1367-2630/14/8/085023

Abstract. We analyse frequency spectra of absolute optical instruments and show that they have very specific properties: the eigenfrequencies form tight groups that are almost equidistantly spaced. We prove this by theoretical analysis and demonstrate by numerically calculated spectra of various examples of absolute instruments. We also show that in rotationally and spherically symmetric absolute instruments a source, its image and the centre of the device must lie on a straight line.

 Online supplementary data available from stacks.iop.org/NJP/14/085023/mmedia

³ Author to whom any correspondence should be addressed.



Content from this work may be used under the terms of the [Creative Commons Attribution-NonCommercial-ShareAlike 3.0 licence](http://creativecommons.org/licenses/by-nc-sa/3.0/). Any further distribution of this work must maintain attribution to the author(s) and the title of the work, journal citation and DOI.

Contents

1. Introduction	2
2. Absolute optical instruments	3
3. Green's function	5
4. Emission and re-absorption of a pulse at the same point	6
5. Emission and absorption of a pulse at different points	9
5.1. Two-dimensional rotationally symmetric absolute instruments	9
5.2. Three-dimensional spherically symmetric absolute instruments	11
5.3. The relation between $h_A(t)$ and $h_B(t)$	12
6. Spectra of absolute optical instruments of the second type	12
7. Re-absorption of the pulse in arbitrary cavities	14
8. Conclusions	15
Acknowledgments	15
References	15

1. Introduction

It is well known that the properties of the semiclassical energy spectrum of a quantum-mechanical system are closely related to the behaviour of the corresponding classical system described by the same Hamiltonian. One example is classical billiard problems (infinite potential wells with various shapes) that exhibit chaotic behaviour in some part of the phase space and regular behaviour in another part. The spectra of quantum versions of these systems have a typical structure consisting of independent sequences of levels, some of which correspond to the chaotic orbits and some to the regular ones. These properties have been investigated in great detail using the theory of Green's functions [1, 2] and asymptotics [3].

The situation in optics is similar. Consider electromagnetic waves in a two-dimensional (2D) optical metallic cavity polarized such that the electric field is perpendicular to the plane of the cavity. Such waves can be described by a scalar wave equation, and the eigenvalue problem for the wavenumber $k = \omega/c$ is completely equivalent to the eigenvalue problem for the energy E of a quantum particle in an infinite potential well of the same shape, with the relation $k^2 = 2mE/\hbar^2$ between E and k . Therefore a similar relationship as in the billiard problem must hold between classical ray propagation in the cavity and the frequency spectrum of its modes.

In optics there exists an additional interesting class of systems possessing a unique property that is rare in mechanics. These devices are called absolute optical instruments (AIs) [4, 5] with the property that the rays in them form closed trajectories for various ray parameters, and often closed paths are formed by all rays. An archetype of an absolute instrument is Maxwell's fish eye, discovered in 1854 by Maxwell [6]. Recently, it has been shown both theoretically [7] and experimentally [8] that this device has the ability to provide subwavelength imaging, beating the diffraction limit. This might open the way to important applications of absolute instruments in microscopy or nanolithography, and the investigation of their wave properties is therefore very desirable. Since in the mechanical problem closed trajectories have a strong influence on the spectrum [2], we can surmise that the spectrum of absolute instruments may also have some interesting general features. In addition, the spectrum can provide much, albeit not all [9, 10],

information about the system. For these reasons, it is of great interest to investigate spectra of absolute instruments and find out whether they share some general properties.

This is the purpose of this paper. Our analysis shows that the eigenfrequency spectra of absolute instruments tend to be composed of regularly spaced groups of densely packed levels. Our results are derived by a different method than was employed for quantum systems [1–3], by investigating pulse propagation in absolute instruments. We confirm our theoretical analysis by numerical calculations of the spectra for several examples of absolute instruments.

The paper is organized as follows. In section 2, we recall properties of absolute instruments and define several types of them; in section 3, we discuss the Green's function of absolute instruments essential for deriving the subsequent results. In section 4, we analyse the emission and absorption of a pulse at the same point and in section 5 at different points, from which we derive a theorem restricting the mutual position of a source and its image. In section 6 we discuss the spectrum of one type of absolute instrument, in section 7 we analyse the emission and absorption of a pulse in arbitrary cavities and in section 8 present the conclusions.

2. Absolute optical instruments

In this section, we recall some properties of AIs. For a more detailed analysis of their general properties and examples, see [4, 5]. We will also make several additional definitions that will be needed for the derivation of the subsequent results.

An AI is a device that images stigmatically (sharply) a 3D region of space within geometrical optics [4]. A stigmatic image of a point A is a point B through which an infinity of rays emerging from A pass. In [5], we have introduced two types of stigmatic images: a strong image that is formed at B by all rays emerging from A into some nonzero solid angle and a weak image formed at B by an infinity of rays emerging from A that constitute, however, a zero solid angle (e.g. they all lie in a plane as in imaging by a stigmatic cylindrical lens).

Since we want to cover both the 2D and 3D situations, we will also generalize the name 'absolute instrument' to the case of 2D light propagation in a plane where, of course, no imaging of 3D regions would make sense. In this situation, an AI is a device that images stigmatically a 2D region of the plane within geometrical optics, and an image formed by all rays emerging into a nonzero angle will be called strong.

We will also define two specific types of AIs. If a point A has a strong image B that is formed by all the rays emerging from A (i.e. rays emerging into the full angle 2π rad in the 2D case or the full solid angle of 4π sr in the 3D case), we will call B a *full image* of A. If a point A has a strong image B that is not full, we will call that image *partial*. A device in which any point has a full image will be called an *AI of the first type*. A device in which just points from some region (not everywhere) have full images will be called an *AI of the second type*. We term the region of points having full images as *Region I* and the region of points having partial images as *Region II*. Of course, there exist absolute instruments that are neither of the first nor of the second type; we will not consider them in this paper.

The archetype of absolute instruments, Maxwell's fish eye [6] mentioned in the introduction, has a spherically symmetric (or, in the 2D case, radially symmetric) refractive index profile $n(r) = 2/(1 + r^2/a^2)$, where r is the radial coordinate and a a length parameter. This device is an AI of the first type as it creates a full image of the whole space, see figure 1(a). By adding a spherical (or, in 2D, a circular) mirror at radius a , one gets a device called

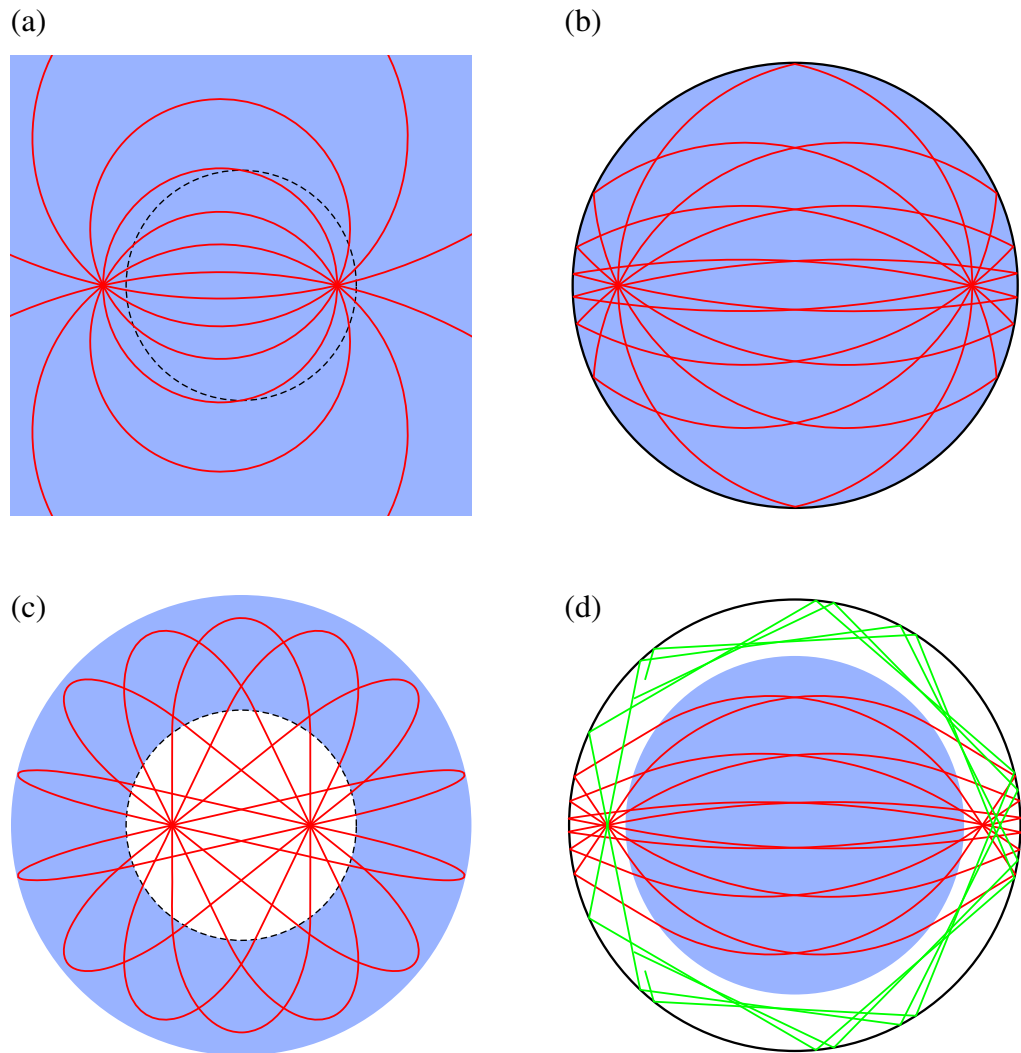


Figure 1. Examples of absolute instruments: (a) Maxwell's fish eye, (b) Maxwell's fish eye mirror, (c) Miñano lens and (d) modified Maxwell's fish eye mirror. The black circles mark the radius a , where in panels (b) and (d) a mirror is placed. The medium in all plots is shown in blue; in panel (d) it occupies Region I only while the refractive index in Region II (white) is unity; the radius of Region I in this particular example is $R = 0.75 a$. Points in Region I have full images, whereas points in Region II have just partial images since some rays (here shown in green) from the source miss the image as well as the medium.

Maxwell's fish eye mirror [7], which is also an AI of the first type, see figure 1(b). Another interesting example is the Miñano lens [5, 11] with a homogeneous region of refractive index $n(r) = 1$ for $r \leq a$ and $n(r) = \sqrt{2a/r - 1}$ for $a \leq r \leq 2a$, see figure 1(c). Recently, a general method for designing AIs with spherical symmetry has been developed that can be used to produce infinitely many different AIs of the first type [5].

An example of an AI of the second type is the modified Maxwell's fish eye mirror [12, 13], see figure 1(d). There, Region I is a full sphere (or, in 2D, a disc) of radius $R < a$ and the rest of the device is occupied by Region II with unit refractive index.

3. Green's function

We will consider waves in a medium with a spatially variable refractive index $n(r)$, and assume throughout this paper that the waves are confined in some way and cannot leak out of the device. This makes the frequency spectrum of the modes discrete. We can achieve this in several ways—by encapsulating the device in a spherical mirror, by employing an imaginary refractive index, which forces the field to be evanescent beyond some radius, or by letting the refractive index go to zero sufficiently fast for $r \rightarrow \infty$ (this is the case of Maxwell's fish eye [14]).

For simplicity, we will consider scalar waves governed by the wave equation

$$\Delta \Psi - \frac{n^2}{c^2} \frac{\partial^2 \Psi}{\partial t^2} = q(\vec{r}, t), \quad (1)$$

where c is the speed of light in vacuum and $q(\vec{r}, t)$ is a function describing the sources of the waves. In the absence of sources ($q = 0$) and for harmonic dependence of Ψ on time, $\Psi(\vec{r}, t) = \psi(\vec{r}) \exp(-i\omega t)$, we obtain for ψ the Helmholtz equation with a variable refractive index

$$\Delta \psi + k^2 n^2 \psi = 0, \quad (2)$$

where $k = \omega/c$. The solution to equation (2) is given by a discrete set of mode functions $\psi_i(\vec{r})$ with the corresponding wavenumbers $k_i = \omega_i/c$. It is easy to show that the mode functions corresponding to different frequencies are orthogonal with respect to the weight function $n^2(\vec{r})$. If we normalize them with respect to this weight function, we obtain a complete orthonormal basis of functions

$$\int_V n^2(\vec{r}) \psi_i^*(\vec{r}) \psi_j(\vec{r}) d\vec{r} = \delta_{ij}, \quad (3)$$

where V denotes the volume of the device.

The retarded Green's function for the wave equation (1) can be found by standard techniques described, for example, in [15] for the case of the scalar wave equation with a constant wave speed. The result is

$$G(\vec{r}, t | \vec{r}_0, t_0) = c^2 \Theta(t - t_0) \sum_i \frac{\sin[\omega_i(t - t_0)]}{\omega_i} \psi_i^*(\vec{r}_0) \psi_i(\vec{r}), \quad (4)$$

where $\Theta(t)$ is the Heaviside step function.

Suppose that there is no wave in the medium at $t = -\infty$, so any wave present later is a result of the action of a source function $q(\vec{r}, t)$. The wave at time t can then be expressed in terms of Green's function (4) as

$$\psi(\vec{r}, t) = \int_V d\vec{r}_0 \int_{-\infty}^t dt_0 q(\vec{r}_0, t_0) G(\vec{r}, t | \vec{r}_0, t_0). \quad (5)$$

Alternatively, at any time t the wave is completely and uniquely described by the set of coefficients $\{c_i(t), i = 1, 2, \dots\}$ of its expansion in terms of mode functions,

$\psi(\vec{r}, t) = \sum_{i=1}^{\infty} c_i(t) \psi_i(\vec{r})$. Using equations (3), (4) and (5), we can express $c_i(t)$ as

$$\begin{aligned} c_i(t) &= \int_V d\vec{r} n^2(\vec{r}) \psi_i^*(\vec{r}) \psi(\vec{r}, t) \\ &= \frac{c^2}{2i\omega_i} \left[e^{i\omega_i t} \int_{-\infty}^t dt_0 e^{-i\omega_i t_0} \int_V d\vec{r}_0 \psi_i^*(\vec{r}_0) q(\vec{r}_0, t_0) \right. \\ &\quad \left. - e^{-i\omega_i t} \int_{-\infty}^t dt_0 e^{i\omega_i t_0} \int_V d\vec{r}_0 \psi_i^*(\vec{r}_0) q(\vec{r}_0, t_0) \right]. \end{aligned} \quad (6)$$

This expression will be useful in the following.

4. Emission and re-absorption of a pulse at the same point

In this section, we derive some important properties of the frequency spectra of absolute instruments of the first type. For this, we will employ the obvious fact that if a point A has a full image at B, then the point B has a full image at A. This way, in any absolute instrument of type 1 any point is a full image of itself: all rays emerging from A will return back to A. From the point of view of wave optics, it should then be possible to emit a pulse at point A and later absorb it at the same point. This way, the point A would serve as both the source of the wave and its absorber (drain) at a later time.

We will consider the absorption to be active in the sense that the absorber does not just respond passively to the field but emits a precisely tailored absorbing pulse to swallow all the previously injected radiation. We will describe both the emission and absorption by a single source function $q(\vec{r}, t) = q_A(\vec{r}, t) = \delta(\vec{r} - \vec{r}_A) h(t)$ that has a peak around the emission time and another peak around the absorption time.

If the pulse is emitted and then re-absorbed, there should be no wave left in the medium for $t \rightarrow \infty$. Therefore all the coefficients $c_i(t)$ should turn to zero at $t = \infty$. Substituting for $q(\vec{r}, t)$ into equation (6), we get for each mode the condition

$$\int_{-\infty}^{\infty} h(t) e^{\pm i\omega_i t} dt = 0. \quad (7)$$

We see that the Fourier components of the source functions at the resonant frequencies (including their negative counterparts) should be zero. This is in fact quite a natural requirement: after the source function q_A dies out, no mode ψ_i should be left excited, which is ensured by the vanishing of the Fourier components of the source function at the resonant frequencies ω_i .

Condition (7) has important consequences for frequency spectra of absolute instruments of the first type. We first give a heuristic argument for this and then proceed to a more rigorous one.

In an AI of the first type, a short pulse emitted from any point A at time $t = 0$ comes back to A from all directions after the time T corresponding to completing a round trip in the instrument. It should therefore be possible to absorb the pulse at A by applying an absorbing pulse at time $t = T$, and the corresponding source function $h(t)$ is hence composed of two wavelets centred around 0 and T . The Fourier transform $\tilde{h}(\omega)$ of such a function h will then have oscillatory behaviour, reminiscent of beats when two tones of a similar frequency are mixed, with the typical distance $\Delta\omega = 2\pi/T$ between zeros of $\tilde{h}(\omega)$. At the same time, we know from equation (7) that $\tilde{h}(\omega)$ should have zeros at the resonant frequencies ω_i . This implies

that the frequencies ω_i should be arranged almost equidistantly with a spacing of approximately $2\pi/T$. However, since in 2D and 3D the density of states increases with increasing frequency, it cannot be single eigenfrequencies but rather their groups that have to be arranged this way, so the spectra can be expected to be highly degenerate, at least approximately.

To derive this heuristic result more rigorously, we proceed in a different way and define a function $\omega(\nu)$ that characterizes the spectrum of such an AI and will be useful for further calculations. To do this, we arrange the eigenfrequencies ω_i in non-decreasing order ($\omega_1 \leq \omega_2 \leq \dots$); an s times repeated value in the sequence corresponds to an s times degenerate level. The function $\omega(\nu)$ is then defined for positive integer values of ν simply by $\omega(\nu) = \omega_\nu$. For non-integer values $\nu > 1$, it is defined by linear interpolation:

$$\omega(\nu) = \omega_i + (\nu - i)(\omega_{i+1} - \omega_i), \quad (8)$$

where i is the integer part of ν . Note that the function $\omega(\nu)$ is continuous and degenerate levels correspond to intervals of constant $\omega(\nu)$. We will also need to define $\omega(\nu)$ for $\nu < 1$. For that, we define a sequence ω_j with $j = 0, -1, -2, \dots$ of negative counterparts of the eigenfrequencies as follows. If the spectrum contains the zero eigenfrequency, i.e. if $\omega_1 = 0$ (such as in Maxwell's fish eye), we define $\omega_j = -\omega_{2-j}$; if it does not (such as in Maxwell's fish eye mirror), we put $\omega_j = -\omega_{1-j}$. We then define $\omega(\nu)$ for all $\nu < 1$ by equation (8). This way, $\omega(\nu)$ is defined for all real ν . In the case of a non-degenerate spectrum, we can also define the inverse function $\nu(\omega)$ by inverting $\omega(\nu)$. If the spectrum is degenerate, then $\nu(\omega)$ is well defined except at the discrete set of degenerate frequencies.

Equipped with the functions $\omega(\nu)$ and $\nu(\omega)$, we choose the source function as follows:

$$h(t) = \frac{1}{\sqrt{2\pi}} \int_{-\infty}^{\infty} \tilde{F}(\omega) (1 - e^{2i\pi\nu(\omega)}) e^{-i\omega t} d\omega, \quad (9)$$

where $\tilde{F}(\omega)$ is some bounded function. The integral makes sense even for a degenerate spectrum since the discrete set of frequencies for which $\nu(\omega)$ is undefined has a zero measure. For the Fourier transform $\tilde{h}(\omega)$ of $h(t)$, it holds that

$$\tilde{h}(\omega) \equiv \frac{1}{\sqrt{2\pi}} \int_{-\infty}^{\infty} h(t) e^{i\omega t} dt = \tilde{F}(\omega) (1 - e^{2i\pi\nu(\omega)}), \quad (10)$$

which turns into zero for integer values of ν , i.e. exactly those for which ω corresponds to some eigenfrequency $\pm\omega_i$, just as required by equation (7). This justifies the particular choice (9) of $h(t)$: conditions (7) are satisfied automatically and it is therefore possible to add energy into the system and then extract all of it again, all by the source function (9). In fact, equation (9) is the most general form of the source function satisfying equation (7).

We will now express the function $h(t)$ in a different way. Denoting the inverse Fourier transform of $\tilde{F}(\omega)$ by $F(t) = 1/\sqrt{2\pi} \int_{-\infty}^{\infty} \tilde{F}(\omega) e^{-i\omega t} d\omega$ and using the fact that a product turns into a convolution when Fourier transformed, we can write equation (9) as

$$h(t) = F(t) - \frac{1}{\sqrt{2\pi}} F(t) * \int_{-\infty}^{\infty} e^{2i\pi\nu(\omega) - i\omega t} d\omega, \quad (11)$$

where the symbol $*$ denotes convolution, $(f * g)(x) = \int_{-\infty}^{\infty} f(x-y)g(y) dy$. Choosing the function $F(t)$ to be localized (say, around $t = 0$), the first term $F(t)$ in equation (11) can be interpreted as the emission pulse and the second term as the absorption pulse. For an AI of the first type we can expect that the absorption pulse will be similarly sharp in time as the emission pulse, because the absolute instrument brings the emitted pulse back to the source after the time

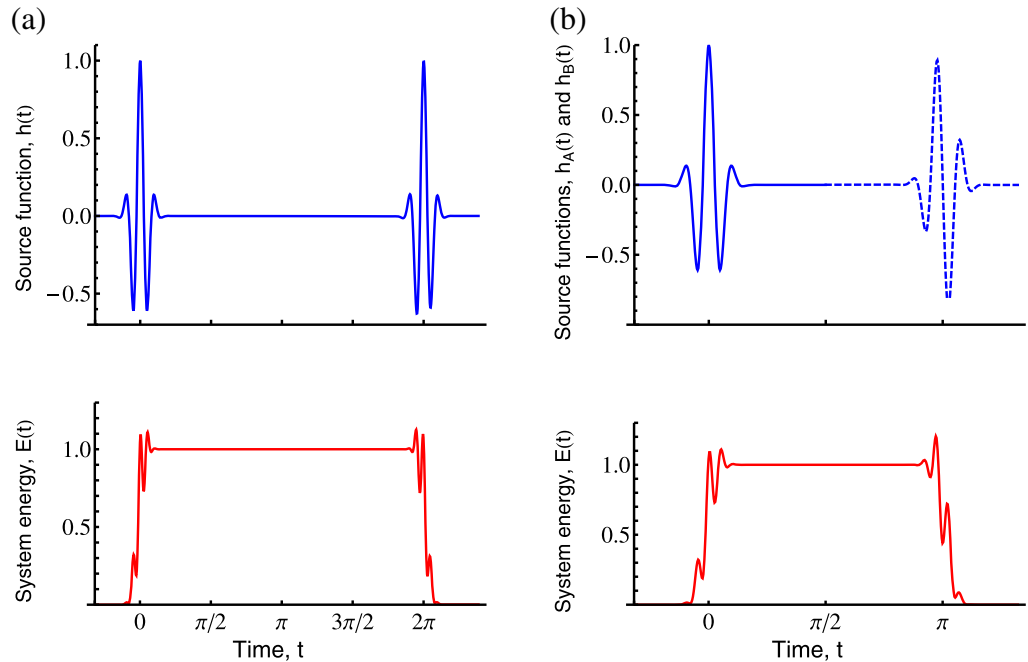


Figure 2. Emission and absorption of a pulse in Maxwell's fish eye mirror with unit radius ($a = 1$) for a Gaussian function $F(t)$ used in equations (11) and (16). In (a), the pulse is emitted and absorbed at the same point A at the radial position $r = 0.5$, whereas in (b) it is emitted at A and absorbed at point B opposite to A. The upper graphs show the real part of the source functions: in (a), it is the function $h(t)$ containing both the emission and absorption pulses; in (b) the emission pulse $h_A(t)$ and absorption pulse $h_B(t)$ are shown by full and dashed lines, respectively. The lower graphs show the energy in the device as a function of time calculated via simulating the wave with the free software Meep. We see that the pulse emitted using a short source function can be completely absorbed by another short source function, which is a specific feature of absolute instruments. Animations 1 and 2 in the supplementary data (available from stacks.iop.org/NJP/14/085023/mmedia) show the corresponding time evolution of the wave in the device.

T . Therefore the integral in equation (11) should be non-zero for a relatively sharp time interval around $t = T$. This is illustrated in figure 2(a) and animations 1 and 2 in the supplementary data (available from stacks.iop.org/NJP/14/085023/mmedia) with the example of Maxwell's fish eye mirror.

To see the implications of this fact, we change the integration variable from ω to ν in the integral in equation (11):

$$I(t) \equiv \int_{-\infty}^{\infty} e^{2i\pi\nu(\omega) - i\omega t} d\omega = \int_{-\infty}^{\infty} \frac{d\omega}{d\nu} \exp[-it\omega(\nu)] \exp(2i\pi\nu) d\nu. \quad (12)$$

The expression (12) has a simple interpretation. It can be regarded as the Fourier component at 'frequency' 2π of the product $d\omega/d\nu \exp[-it\omega(\nu)]$ with time t playing the role of a parameter.

Now, if $I(t)$ is non-zero only for a narrow interval of t around $t = T$, the function $\omega(\nu)$ should essentially be linear with the slope $2\pi/T$.

On the other hand, the density of states in both 2D and 3D grows with frequency, so strictly speaking, $\omega(\nu)$ cannot simply be linear but must grow more slowly on average—for a 2D device it grows on average as a square root and in 3D as a cubic root. The solution of this seeming discrepancy lies in the term $d\omega/d\nu$. Imagine that $\omega(\nu)$ is linear with the slope $2\pi/T$ on some intervals of ν (bounded by integer values of ν) and constant on other intervals. Then the constant intervals will not contribute to $I(t)$ because $d\omega/d\nu = 0$ for them, and the remaining intervals of linear dependence $\omega(\nu)$ will ensure that $I(t)$ is non-zero only for a narrow interval of t around $t = T$. This means, as we have already shown heuristically, that the frequency spectrum of an absolute instrument should be highly degenerate, with spaces of $2\pi/T$ between the groups.

However, an absolute instrument that behaves perfectly within geometrical optics may not behave perfectly within wave optics, especially for low frequencies. Therefore the expected degeneracy of frequency spectra will in general hold only asymptotically for high frequencies as one approaches the geometrical optics limit. In other words, the spectrum of AIs of the first type has to be only ‘approximately degenerate’—the frequencies ω_i should form groups of tightly packed levels with spaces of approximately $2\pi/T$ between the groups.

This general behaviour of the spectrum of AIs is demonstrated in three examples in figures 3(a)–(c), and contrasted with a device that is not an AI—a square cavity with a constant refractive index surrounded by perfect mirrors. The spectrum is represented by the function $\omega(\nu)$. The specific character of the spectra of AIs is obvious.

5. Emission and absorption of a pulse at different points

In this section, we will consider AIs where a pulse emitted from one point can be absorbed at another point. Using similar considerations as in the previous section, this will allow us to derive conditions for relative positions of a source and its image in spherically (in 3D) and rotationally (in 2D) symmetric absolute instruments of the first type, and the spectral properties that follow from that.

Let the pulse be emitted from point A (a source) and absorbed at another point B, which serves as an active drain. We will describe the emission and absorption by source functions $q_A(\vec{r}, t) = \delta(\vec{r} - \vec{r}_A)h_A(t)$ and $q_B(\vec{r}, t) = \delta(\vec{r} - \vec{r}_B)h_B(t)$, respectively. In a similar way as in section 4, we find from the requirement that $c_i(t)$ should vanish for $t \rightarrow \infty$ under the following conditions:

$$\int_{-\infty}^{\infty} [\psi_i^*(\vec{r}_A)h_A(t) + \psi_i^*(\vec{r}_B)h_B(t)] e^{\pm i\omega_i t} dt = 0. \quad (13)$$

In the following, we will treat separately the cases of two and three dimensions.

5.1. Two-dimensional rotationally symmetric absolute instruments

Let us consider first the 2D situation. Due to the rotational symmetry of the device, the generalized Helmholtz equation (2) can be separated into polar coordinates (r, φ) and each mode can be expressed as $e^{im\varphi}R(r)$ with an integer m (we will call this number an *angular mode number*) and a suitable function $R(r)$. Let us take a pair of modes with the same $R(r)$ and opposite values of m , denote them by $\psi_{\pm} = e^{\pm im\varphi}R(r)$ and their frequency by ω . We also

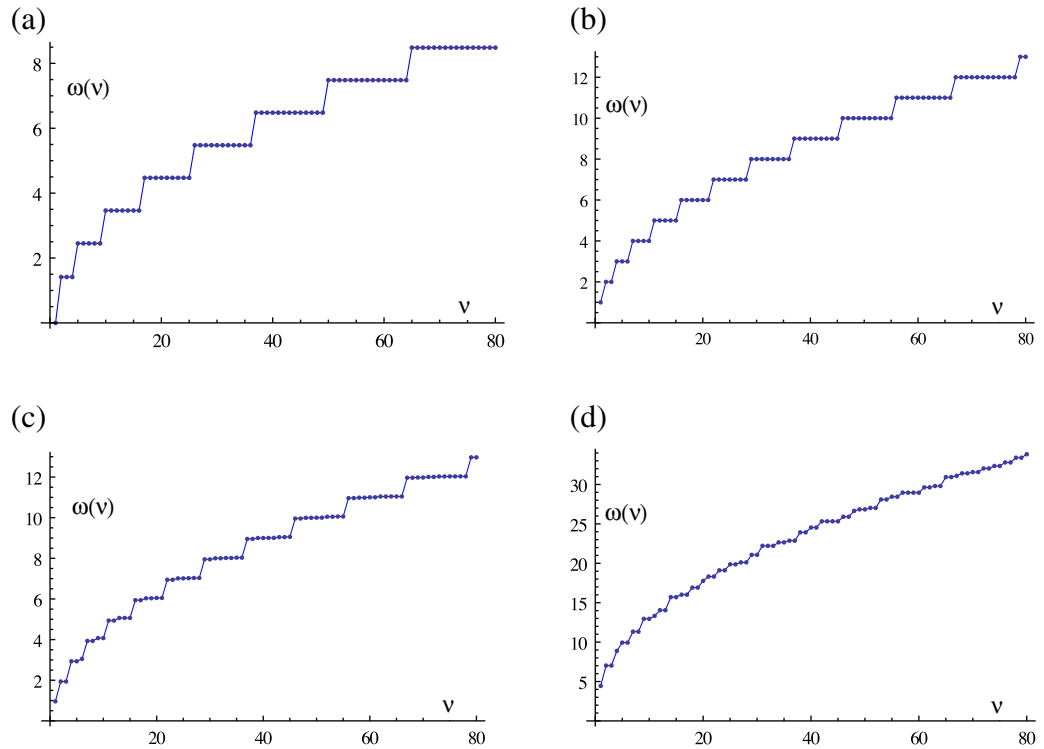


Figure 3. Comparison of spectra of 2D absolute instruments represented by the function $\omega(v)$ with the spectrum of a non-AI. In all cases the speed of the waves and the radius a are equal to unity. (a) Maxwell's fish eye, (b) Hooke index profile $n(r) = \sqrt{2 - r^2}$ with concentric elliptical ray trajectories and (c) Miñano lens. In (b) and (c), a region of purely imaginary index was added beyond the radius $\sqrt{2}$ and 2, respectively, that is inaccessible for light rays but evanescent waves can be formed in it. (d) Spectrum of a unit square cavity surrounded by perfect mirrors, which is not an AI. In (a)–(c), the period of a pulse round trip is $T = 2\pi$; therefore the spacing of the frequency groups asymptotically approaches $\Delta\omega = 2\pi/T = 1$. The spectra were calculated by numerically solving the radial part of equation (2) after separating the angular variable.

denote radial positions and polar angles of points A, B by (r_A, φ_A) and (r_B, φ_B) , respectively. We then write condition (13) for the mode ψ_+ , multiply it by the factor $\exp(i|m|\varphi_A)$ and subtract it from the condition for the mode ψ_- multiplied by the factor $\exp(-i|m|\varphi_A)$. As a result, terms involving the function h_A cancel and we are left with the condition

$$R^*(r_B) \sin[|m|(\varphi_B - \varphi_A)] \int_{-\infty}^{\infty} h_B(t) e^{\pm i\omega t} dt = 0. \quad (14)$$

This condition has important consequences. First of all, since the radial position r_B can be arbitrary, and we cannot assume anything particular about the function $h_B(t)$, then $\sin[|m|(\varphi_B - \varphi_A)]$ must vanish for all m , which implies that either $\varphi_B = \varphi_A$ or $\varphi_B = \varphi_A \pm \pi$. This way, the source, its image and the centre of symmetry of the lens must lie on a straight line. Remarkably,

this feature of absolute instruments was proved in [5] by a completely different approach based on geometrical optics.

To derive the properties of the spectrum, we will use a general property of AIs that holds not only for AIs of the first or second type, but for all AIs that create strong images. In particular, it was shown in [5] that the radial positions of the source and its image satisfy either the relation $r_A = 1/r_B$ or $r_A = r_B$. The first case corresponds to generalized Maxwell's fish eyes and we will not discuss it here.

We will focus on the second situation when $r_A = r_B$, which corresponds to a much more general class of AIs [5], and discuss the two possibilities $\varphi_B = \varphi_A$ and or $\varphi_B = \varphi_A \pm \pi$ separately. The first case $\varphi_B = \varphi_A$ implies $A = B$, which takes us back to the situation of emission and re-absorption of the pulse at the same point discussed in the previous section. The second case $\varphi_B = \varphi_A \pm \pi$ corresponds to the image located opposite the source, viewed from the centre of the lens. Then it holds that $\psi_i^*(\vec{r}_A) = (-1)^{m_i} \psi_i^*(\vec{r}_B)$, where m_i denotes the angular mode number corresponding to the i th mode. Inserting this into equation (13), we obtain the condition

$$\int_{-\infty}^{\infty} [h_A(t) + (-1)^{m_i} h_B(t)] e^{\pm i\omega_i t} dt = 0. \quad (15)$$

Using now the result from the previous section, namely that the frequency spectrum of an AI of the first type is highly degenerate (at least approximately), we see that it is not possible to have two modes i, j with almost the same frequency but with their angular mode numbers m_i, m_j of a different parity; otherwise the Fourier components at ω_i of the functions $h_A(t)$ and $h_B(t)$ would have to be zero separately, which we do not assume. Hence, we see that in AIs of the first type where the source and its image are opposite across the centre, the (approximately) degenerate groups of frequencies correspond to angular mode numbers of the same parity. This causes a typical structure of the spectrum of 2D AIs of this type: the numbers of levels in the (approximately) degenerate groups grow by one as they correspond to the following options for m : (0), (-1, 1), (-2, 0, 2), (-3, -1, 1, 3) etc. This is illustrated in figures 3(b) and (c). On the other hand, for AIs that do not have an image opposite the source, there is no restriction for the angular mode numbers m related to the (approximately) degenerate levels. Hence, the level scheme is (0), (-1, 0, 1), (-2, -1, 0, 1, 2) etc, and the numbers of levels in the groups hence grow by two. This is illustrated in figure 3(a) for the example of Maxwell's fish eye.

5.2. Three-dimensional spherically symmetric absolute instruments

For 3D spherically symmetric AIs, we can also prove that the source A, its image B and the lens centre O must lie on a straight line; we proceed in a similar way as for the 2D situation. Modes are now separable in spherical coordinates as $Y_{lm}(\theta, \varphi) R(r) \propto P_l^m(\cos \theta) e^{im\varphi} R(r)$ with Y_{lm} and P_l^m being the spherical harmonic and associated Legendre polynomial, respectively. We choose the z -axis to be perpendicular to the plane OAB, which places the source and its image on the equator. Applying then the same argumentation as above to the modes with the same parity of l, m (the others vanish on the equator), in particular equation (14), we find that the points O, A and B lie on a straight line.

Regarding the level scheme for spherically symmetric AIs, we note that in all spherically symmetric media there is a degeneracy with respect to the angular mode number m . This is caused by the fact that $Y_{lm}(\theta, \varphi)$ are eigenfunctions of the Laplacian with the eigenvalues $l(l+1)$

depending on l but not m . Our results derived above therefore mean that in 3D AIs of the first type there is additionally a strong approximate degeneracy with respect to l .

5.3. The relation between $h_A(t)$ and $h_B(t)$

What remains to be discussed is the relationship between the source functions $h_A(t)$ and $h_B(t)$ in the case of emission and absorption of a pulse at different points A (source) and B (drain). As we have seen, in this situation points A and B are opposite each other (with the exception of the generalized Maxwell's fish eye which we do not consider here). The functions $h_A(t)$ and $h_B(t)$ then have to satisfy condition (15), which can be ensured by putting

$$h_A(t) = F(t), \quad h_B(t) = -\frac{1}{\sqrt{2\pi}} F(t) * \int_{-\infty}^{\infty} e^{i\pi[2\nu(\omega)+M(\omega)]-i\omega t} d\omega. \quad (16)$$

Here the function $M(\omega)$ is defined as follows. If ω lies within some of the groups of tightly spaced frequency levels of the spectrum we have discussed, $M(\omega)$ takes an integer value of the same parity as the parity of the angular mode numbers m corresponding to that group (as we have seen, the parities of the numbers m are the same for all levels within the group). When going from one group to the next, the value of M grows by unity. In the regions between the groups, the value $M(\omega)$ is obtained by interpolation. It is not difficult to see that this choice of functions $h_A(t)$ and $h_B(t)$ automatically satisfies condition (15) and therefore the pulse emitted at A will be absorbed at B. At the same time, the function $M(\omega)$ will be close to linear because of the general character of the spectra of AIs we have derived. This will then ensure that for a short pulse $h_A(t)$ the pulse $h_B(t)$ will also be short. This situation is illustrated in figure 2(b) for the example of Maxwell's fish eye mirror.

6. Spectra of absolute optical instruments of the second type

In the previous sections, we have analysed spectra of absolute instruments of the first type. Now we turn our attention to AIs of the second type. In them, for points A from Region I (see section 2) all rays emerging from A reach its image B, but for points A from Region II some rays emerging from A reach the image B and some do not. A typical example is a modified Maxwell's fish eye mirror discussed in section 2 and in detail in [12].

To derive the properties of the spectrum, we can proceed in exactly the same way as in the two previous sections for points from Region I. However, for points from Region II we can no longer claim that a pulse emitted from A can completely be absorbed at its image B because some rays from A simply miss B. This means that modes that have a significant contribution in Region I must follow the rules derived above, i.e. form tight groups with approximately equidistant spacing. However, modes whose wavefunction ψ_i practically turns to zero in Region I do not have to obey these rules because they simply cannot 'spoil' imaging of Region I. Therefore the spectrum will be composed of two sequences of levels: one approximately degenerate and regularly spaced and the other one essentially random. This is very similar behaviour to that of the levels of quantum billiards [1–3] where different sequences of levels also coexist, some of which correspond to chaotic orbits and some to regular ones.

This typical behaviour is illustrated in figure 4 for the modified Maxwell's fish eye mirror. There the eigenfrequencies are shown as functions of the radius R of Region I with different colours distinguishing different angular mode numbers m . The curve becomes dashed for such

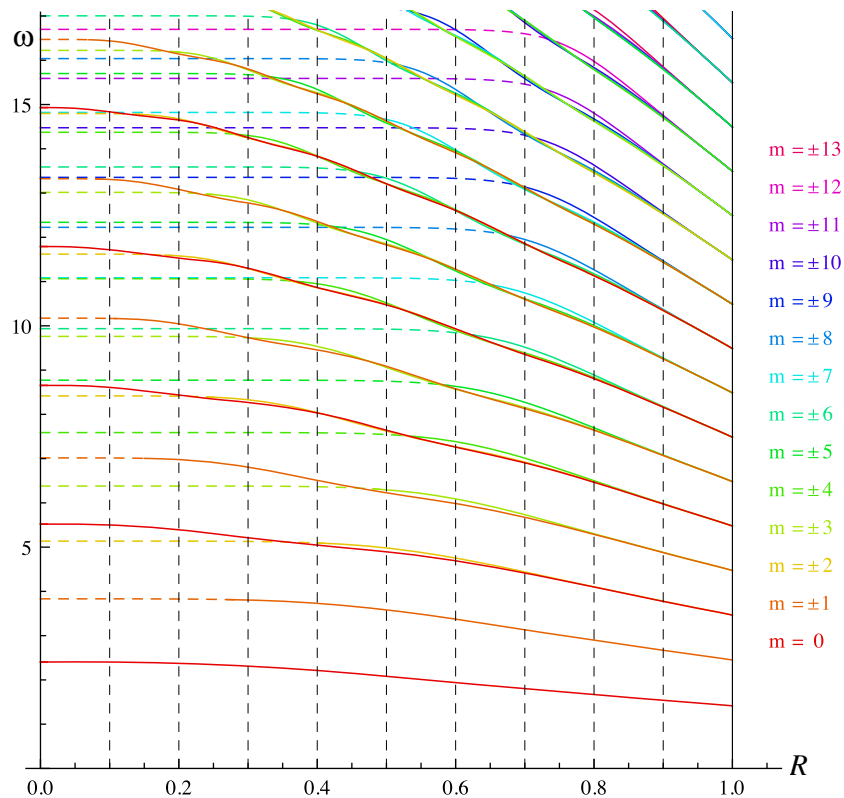


Figure 4. Spectrum of AI of the second type—the 2D modified Maxwell’s fish eye mirror of unit radius ($a = 1$) and different radii R of the medium. The radius R is on the horizontal axis, the eigenfrequencies on the vertical axis and c is set to unity. Different colours distinguish different angular mode numbers m . The dashed parts of the lines mark the situation when the corresponding mode has large enough angular momentum so as not to penetrate into Region I ($r < R$); such modes are confined to the homogeneous Region II ($R < r \leq 1$) and therefore do not spoil the full imaging in Region I. The intersections of the full lines with the lines of constant R have the character of the spectrum of AIs of the first type. The spectrum is alternatively represented in animation 3 in the supplementary data (available from stacks.iop.org/NJP/14/085023/mmedia).

an interval of R where its angular mode number m is larger than $\omega R/c$; this condition guarantees that the wave has large enough angular momentum so as not to penetrate into Region I (strictly speaking, the wave does penetrate but it is evanescent in that region). The intersections of the full lines with the lines of constant R show only the spectrum of those modes that penetrate into Region I, and they therefore have the character of the spectra of AIs of the first type. Note also that the dashed parts of the lines are almost horizontal. This is because when a mode does not penetrate into Region I, it hardly gets shifted when the radius R of this region is changed.

Another useful aspect of figure 4 can be seen when looking at it without paying attention to whether the lines are dashed or not. Then we see a smooth transition from the spectrum of an AI at $R = 1$ (Maxwell’s fish eye mirror) to the spectrum of a non-AI at $R = 0$ (a homogeneous disc

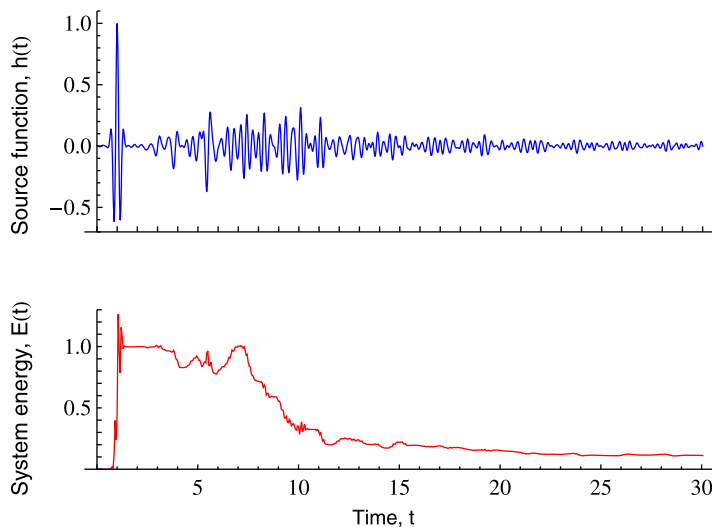


Figure 5. Emission and re-absorption of a pulse at the centre of a square cavity. The upper graph shows the real part of the source function $h(t)$ for a Gaussian function $F(t)$ from equation (11), the lower graph shows the energy in the device as a function of time. Because of the irregular character of the spectrum, the short emission pulse is followed by a very long absorbing tail (the graph shows just a part of it); it therefore takes a long time to extract the energy from the system, unlike in AIs. Animation 4 in the supplementary data (available from stacks.iop.org/NJP/14/085023/mmedia) shows the corresponding time evolution of the wave.

surrounded by a mirror). An animated illustration of the spectrum can be seen in animation 3 in the supplementary data (available from stacks.iop.org/NJP/14/085023/mmedia).

7. Re-absorption of the pulse in arbitrary cavities

To see from a still different perspective the contrast between absolute instruments and devices that are far from AIs, we will investigate the possibility of emission and re-absorption of a pulse in a cavity that is not an absolute instrument. The results of section 4, in particular the form of the source function (11), are still valid. The difference is that now a short pulse described by a well-localized function $F(t)$ becomes very wide when convoluted with the function $I(t)$ from equation (12). This is caused by the random character of the spectrum, in contrast to the regular spectrum of AIs, which results in many different values of the slope of the function $\omega(\nu)$ in the exponent in equation (12) and thus to a wide character of the function $I(t)$.

We demonstrate this with an example of a square cavity whose spectrum is shown in figure 3(d). Figure 5 shows an example of the source function $h(t)$ satisfying equation (7) and corresponding to a sharp emission pulse $F(t)$. We see that the absorption part of $h(t)$ has a very long tail and the absorption thus takes a very long time. Figure 5 also shows for this particular $h(t)$ the dependence of the total energy in the system as a function of time which was calculated by running a finite difference time domain (FDTD) simulation of the wave in the cavity (performed with the free software Meep). We see that the energy increases quickly when

the first peak corresponding to the function $F(t)$ comes, and then gradually decreases with time as the absorbing source function $F(t) * I(t)$ acts; the absorption takes a very long time now. Animation 4 in the supplementary data (available from stacks.iop.org/NJP/14/085023/mmedia) shows the evolution of the wave in the cavity in this situation as well as the gradually decreasing energy in the system.

8. Conclusions

In this paper we have analysed properties of eigenfrequency spectra of AIs. By considering the process of emission, propagation and absorption of a pulse, we have shown that the spectra of AIs of the first type have a typical structure of approximately equidistantly spaced, tightly packed groups of levels. For AIs of the second type, there exist additional levels that do not obey this rule; they correspond to modes that do not penetrate to the region whose points have full images. We have also derived in a different way the previously known result that in rotationally and spherically symmetric media the source, its image and the centre of the device must lie on a straight line.

Our research opens many questions to be answered. For example, it would be worth exploring the asymptotic behaviour of the groups of levels for large frequencies, in particular the extensions and spacings of the groups. Another interesting question is related to reshaping of a pulse as a result of the Gouy phase, which occurs in 2D AIs and can most likely be explained by the properties of their spectra in a similar way as described in [16] for a different system. It would also be worth exploring how perturbations (imperfections of the refractive index profile or of the shape of the mirrors, etc) would influence the spectrum and how this is related to the corresponding ray-optical aberrations introduced this way.

Acknowledgments

We thank Michal Lenc for his comments. TT acknowledges support from grant no. P201/12/G028 of the Grant Agency of the Czech Republic and from the QUEST programme grant of the Engineering and Physical Sciences Research Council. AD acknowledges support from grant no. R-263-000-690-112 of Singapore's Ministry of Education Tier 1 Academic Research Fund.

References

- [1] Gutzwiller M C 1970 *J. Math. Phys.* **11** 1791
- [2] Gutzwiller M C 1971 *J. Math. Phys.* **12** 343
- [3] Berry M V 1984 *J. Phys. A: Math. Gen.* **17** 2413
- [4] Born M and Wolf E 2006 *Principles of Optics* (Cambridge: Cambridge University Press)
- [5] Tyc T, Herzánová L, Šarbort M and Bering K 2011 *New J. Phys.* **13** 115004
- [6] Maxwell J C 1854 *Camb. Dublin Math. J.* **8** 188
- [7] Leonhardt U 2009 *New J. Phys.* **11** 093040
- [8] Ma Y G, Sahebdivan S, Ong C K, Tyc T and Leonhardt U 2011 *New J. Phys.* **13** 033016
- [9] Kac M 1966 *Am. Math. Mon.* **73** 1
- [10] Giraud O and Thas K 2010 *Rev. Mod. Phys.* **82** 2213

- [11] Miñano J C 2006 *Opt. Express* **14** 9627
- [12] Ma Y G, Sahebdivan S, Ong C K, Tyc T and Leonhardt U 2012 *New J. Phys.* **14** 025001
- [13] Demkov Y N and Ostrovsky V N 1971 *Sov. Phys.—JETP* **33** 1083
- [14] Luneburg R K 1964 *Mathematical Theory of Optics* (Berkeley: University of California Press)
- [15] Morse P and Feshbach H 1953 *Methods of Theoretical Physics* (New York: McGraw-Hill)
- [16] Tyc T 2012 *Opt. Lett.* **37** 924